A 2,300-year-long annually resolved record of the South American summer monsoon from the Peruvian Andes

Broxton W. Bird[a,1,2], Mark B. Abbott[a], Mathias Vuille[b], Donald T. Rodbell[c], Nathan D. Stansell[a,1], and Michael F. Rosenmeier[a]

[a]Department of Geology and Planetary Science, University of Pittsburgh, 4107 O'Hara Street, Pittsburgh, PA 15260; [b]Department of Atmospheric and Environmental Sciences, University at Albany, State University of New York, 1400 Washington Avenue, Albany, NY 12222; and [c]Geology Department, Union College, 807 Union Street, Schenectady, NY 12308

Decadal and centennial mean state changes in South American summer monsoon (SASM) precipitation during the last 2,300 years are detailed using an annually resolved authigenic calcite record of precipitation $\delta^{18}O$ from a varved lake in the Central Peruvian Andes. This unique sediment record shows that $\delta^{18}O$ peaked during the Medieval Climate Anomaly (MCA) from A.D. 900 to 1100, providing evidence that the SASM weakened considerably during this period. Minimum $\delta^{18}O$ values occurred during the Little Ice Age (LIA) between A.D. 1400 and 1820, reflecting a prolonged intensification of the SASM that was regionally synchronous. After the LIA, $\delta^{18}O$ increased rapidly, particularly during the current warm period (CWP; A.D. 1900 to present), indicating a return to reduced SASM precipitation that was more abrupt and sustained than the onset of the MCA. Diminished SASM precipitation during the MCA and CWP tracks reconstructed Northern Hemisphere and North Atlantic warming and a northward displacement of the Intertropical Convergence Zone (ITCZ) over the Atlantic, and likely the Pacific. Intensified SASM precipitation during the LIA follows reconstructed Northern Hemisphere and North Atlantic cooling, El Niño-like warming in the Pacific, and a southward displacement of the ITCZ over both oceans. These results suggest that SASM mean state changes are sensitive to ITCZ variability as mediated by Western Hemisphere tropical sea surface temperatures, particularly in the Atlantic. Continued Northern Hemisphere and North Atlantic warming may therefore help perpetuate the recent reductions in SASM precipitation that characterize the last 100 years, which would negatively impact Andean water resources.

oxygen isotopes | varves | tropical hydroclimate

Recent work documenting the timing and geographic patterns of sub-centennial-scale Asian (1) and African (2) monsoon variability has advanced our understanding of late Holocene Northern Hemisphere (NH) monsoon systems; however, our knowledge of Southern Hemisphere monsoon variability remains limited. This is particularly true for the South American summer monsoon (SASM), the largest monsoon system in the Southern Hemisphere. Documenting the timing, direction, and magnitude of decadal to centennial changes in the SASM in the past will help determine the causes and relative importance of factors that influence monsoons and ultimately improve our knowledge of the climate system.

Previous paleoclimate studies in tropical South America show that over millennial time scales orbitally driven latitudinal changes in the Intertropical Convergence Zone (ITCZ), tropical continental convection and North Atlantic sea surface temperatures (SST) play important roles in driving SASM fluctuations (3, 4). However, the paucity of high-resolution Holocene hydroclimate records from tropical South America has hindered an evaluation of the role of these processes on SASM variability at decadal to centennial time scales. Here, we present an annually resolved reconstruction of the isotopic composition of tropical

South American precipitation as preserved in authigenic sedimentary calcite from Laguna Pumacocha, a varved alpine lake in the central Peruvian Andes. This unique archive documents subdecadal to centennial-scale variations in SASM precipitation over the last 2,300 years and provides insight into how this system responded to abrupt climate change during the late Holocene.

Study Site

Laguna Pumacocha is a small, high-altitude lake in the eastern Peruvian Andes set in a cirque basin at 4,300 m above sea level (asl) (10.70 °S, 76.06 °W) whose geological, morphological and limnological characteristics make it well-suited for archiving SASM variability in its sedimentary record (Fig. 1 and Fig. S1). The relatively small watershed has an area of only 1.7 km^2 and is surrounded by headwalls that rise to nearly 4,600 m asl. Jurassic marine limestones of the Chambará Fm. comprise the underlying bedrock and supply significant quantities of dissolved HCO_3^- and Ca^{2+} to the lake, maintaining a surface pH of approximately 8, an average alkalinity of 161 mg/L HCO_3^- and saturation with respect to calcite throughout the year. Authigenic calcite comprises between 22 and 38% of the sediment by weight and is likely formed when enhanced biological productivity draws down dissolved CO_2, increasing the lake's alkalinity and pH and initiating calcite precipitation. Scanning electron microscope images of the Pumacocha sediments show that the calcite crystals are euhedral with no apparent contamination by detrital limestone (Fig. S2). This is likely because the lake is flanked on all sides by a broad marshy zone that acts as a natural sediment trap for allochthonous material that might otherwise be washed into the lake during storm events (Fig. S1).

The 23.5-m deep Pumacocha lake basin has a large volume (1.37×10^6 m^3) despite its small surface area (0.09 km^2) and is characterized by steeply sloping sides that drop off rapidly to a flat bottom (Fig. S1). These features contribute to water column stability, which results in permanent stratification and anoxic conditions below 8–12-m water depth. Persistent deepwater anoxia has resulted in the near perfect preservation of millimeter-scale couplets in the upper 176.2 cm of the 579.0-cm Holocene-length record (Fig. S2). These couplets are composed of sub-millimeter-scale laminations of authigenic calcite and diatom-rich organic
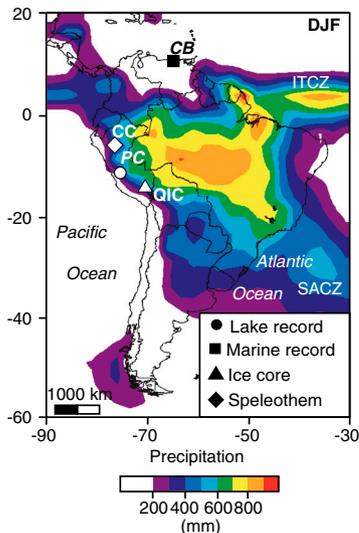
GEOLOGY

Fig. 1. Map of South America showing the locations of records discussed in the text (CB, Cariaco Basin; CC, Cascayunga Cave; PC, Pumacocha; QIC, Quelccaya Ice 557 Cap). Regions with precipitation >200 mm during the austral summer (December–February) are colored. Precipitation maxima over the oceans are related to low-level convergence within the ITCZ and the South Atlantic Convergence Zone (SACZ). Those over South America are associated with the SASM.

matter and were identified as varves based on the agreement between couplet counts, ^{137}Cs and accelerator mass spectrometry (AMS) ^{14}C ages (Fig. 2 and Tables S1 and S2). The varves extend uninterrupted from A.D. 840 to 2007, providing strong temporal constraints on the Medieval Climate Anomaly (MCA), Little Ice Age (LIA), and current warm period (CWP) in the Pumacocha record and allowing comparison with other high-resolution paleoclimate reconstructions.

Results and Discussion

The following discussion documents the close relationship between oxygen isotope values in precipitation ($\delta^{18}O_{precp}$) and lake water ($\delta^{18}O_{lw}$) and sedimentary calcite ($\delta^{18}O_{cal}$) from Pumacocha. We show that Pumacocha $\delta^{18}O_{lw}$ reflects variability in $\delta^{18}O_{precp}$ and that this variability is recorded by the $\delta^{18}O_{cal}$ of authigenic calcite that is precipitated from the lake's water column each year, forming an annually resolved sedimentary archive of SASM intensity. When compared with regional and global paleoclimate records, the Pumacocha $\delta^{18}O_{cal}$ record provides insight into SASM precipitation variability on subdecadal to
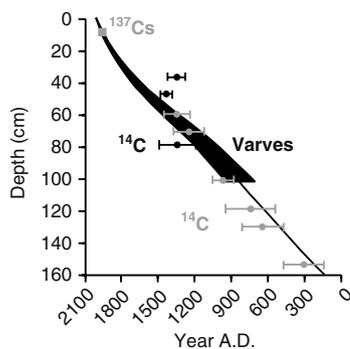
Fig. 2. Age–depth relationships for the Pumacocha record over the last 2,300 years. The gray box demarcates the A.D. 1963 ^{137}Cs peak. Varve ages are shown in black with the 1% cumulative error. AMS ^{14}C ages are represented by gray circles with error bars. Radiocarbon ages that were reversed and excluded from the age model are shown with black circles and error bars. The age–depth model is based on the equation of a 4th order polynomial fit to the AMS ^{14}C ages and anchored to the varve ages.

centennial time scales and during abrupt late Holocene climate events, including the MCA, which is not well documented by the currently available paleoclimate records.

Hydrology and Hydrology and $\delta^{18}O_{precp}$. Pumacocha is the uppermost lake in a topographically isolated catchment with limited groundwater reserves and no fluvial input. As a result, the lake's hydrologic mass balance is dominated by precipitation. Data from the closest weather station in Cerro de Pasco (10.68 °S, 76.25 °W; 4330 m asl) show that regional precipitation averages 1,000 mm yr^{-1} with approximately 60% occurring between December and March during the monsoon season. From these data we estimate that precipitation over the Pumacocha watershed averages approximately 1.67×10^6 m^3 yr^{-1}. This is approximately 23% greater than the total lake volume (1.36×10^6 m^3), thereby maintaining hydrologically open conditions and a surface water residence time of less than a year. As a result, the influence of evaporation on the lake's hydrologic and isotopic mass balances is minimal, a point illustrated by $\delta^{18}O$ and δD measurements on 27 monthly lake water samples collected at Pumacocha between August 2006 and July 2008 (Fig. 3 and Fig. S3). These samples constrain a local meteoric water line (LMWL) that is offset from, but parallel to, the global meteoric water line (GMWL; Table S3). This indicates that the isotopic composition of the lake water reflects seasonal variation in $\delta^{18}O_{precp}$ free from the effects of evaporation. If Pumacocha surface waters were influenced by evaporation, they would plot along the local evaporation line (LEL), which is constrained by water samples from closed basin lakes in the region that are sensitive to evaporation (Fig. 3). This LEL is oblique to the GMWL and LMWL and intersects the LMWL at a $\delta^{18}O$ value of $-13.6‰$. Additional support for the limited role of evaporation is provided by the close agreement between annual mean $\delta^{18}O_{lw}$ ($-13.0‰$) and modeled annual mean $\delta^{18}O_{precp}$ ($-12.9‰ \pm 1.5$) at Pumacocha (Table S4; refs. 5, 6). These data support the contention that Pumacocha $\delta^{18}O_{lw}$ reflects $\delta^{18}O_{precp}$ and that other influences on $\delta^{18}O_{lw}$ are negligible. The monthly water samples also record a strong seasonal cycle,
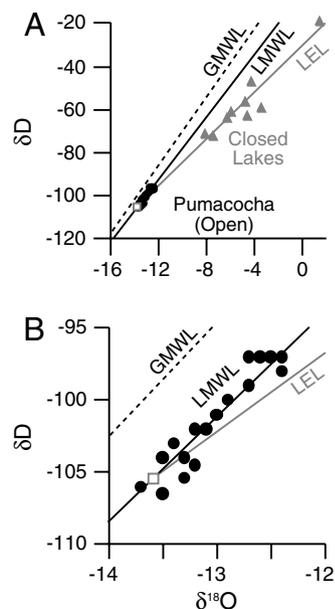
Fig. 3. (A) Surface water samples from Pumacocha (black circles) and regional hydrologically closed basin lakes (gray triangles). Pumacocha surface water samples plot along a LMWL (black line) that parallels the GMWL (dashed line). Regional lakes with closed basin hydrologies plot along a LEL (gray line), which is oblique to both the LMWL and the GMWL and intersects the LMWL at $-13.6‰$ $\delta^{18}O$ (VSMOW; gray square). (B) Same as in A but expanded to illustrate seasonal isotopic variability in the Pumacocha surface water.

indicating that $\delta^{18}O_{lw}$ responds rapidly to changes in $\delta^{18}O_{precip}$ and is sensitive to variations in $\delta^{18}O_{precip}$ (Fig. S3). No relationship was observed between $\delta^{18}O_{lw}$ and air, or lake-surface temperature, which is consistent with work that shows the amount of precipitation and rainout along the trajectory of an air mass are the primary factors that determine $\delta^{18}O_{precip}$ (7).

Pumacocha $\delta^{18}O_{cal}$ and $\delta^{18}O_{precip}$. Modern limnological data from Pumacocha demonstrate a clear relationship among $\delta^{18}O_{lw}$, $\delta^{18}O_{cal}$, and $\delta^{18}O_{precip}$. Authigenic calcite was collected from littoral vegetation at Pumacocha in August 2006 and May 2008, and from deepwater sediment traps deployed between August 2006 and May 2007. When converted to Vienna standard mean ocean water (VSMOW) for comparison with $\delta^{18}O_{lw}$, the annual and three-year-average $\delta^{18}O_{cal}$ values are identical within error to measured mean annual $\delta^{18}O_{lw}$ (Table S4). This indicates that the calcite is precipitated in isotopic equilibrium with Pumacocha lake water and that $\delta^{18}O_{cal}$ measurements can be used to reconstruct past $\delta^{18}O_{lw}$ variability. Considering the evidence that $\delta^{18}O_{lw}$ tracks $\delta^{18}O_{precip}$, the correspondence between $\delta^{18}O_{lw}$ and $\delta^{18}O_{cal}$ supports using down-core $\delta^{18}O_{cal}$ measurements as a proxy for reconstructing $\delta^{18}O_{precip}$. Although we recognize that the links among $\delta^{18}O_{cal}$, $\delta^{18}O_{lw}$, and $\delta^{18}O_{precip}$ are empirical, the modern observational data support this working model as a reasonable first-order approximation.

Temperature Effect on Pumacocha $\delta^{18}O_{cal}$. Modern limnological and paleoclimate data suggest that temperature has a minor influence on the integrated $\delta^{18}O_{cal}$ signal at Pumacocha. Sediment trap $\delta^{18}O_{cal}$ averaged $-12.8\permil$ and varied by $0.8\permil$, which is about twice that attributable to temperature-controlled fractionation during calcite formation. On longer time scales, $\delta^{18}O_{cal}$ varied by up to $2\permil$ between the LIA and CWP (Fig. 4A). Accounting for temperature-controlled oxygen isotope fractionation during the formation of precipitation from water vapor ($+0.6\permil\,°C^{-1}$; ref. 8) and calcite from lake water ($-0.22\permil\,°C^{-1}$; ref. 9), a $2\permil$ shift requires a $5.5\,°C$ temperature change. This far exceeds

estimates of South American LIA cooling inferred from glacial equilibrium line altitude changes in Bolivia (1.1 to 1.2 °C; ref. 10) and lacustrine temperature reconstructions based on changes in lake productivity in central Chile (0.7 to 0.9 °C; ref. 11). Although a 0.7 to 1.2 °C cooling could account for 0.3 to 0.5‰ (15 to 25%) of the Pumacocha $\delta^{18}O_{cal}$ shift between the LIA and the CWP, the remaining variance is unexplained by temperature. These modern limnological and paleoclimate data suggest that temperature is, and has been, a minor influence on the integrated $\delta^{18}O_{cal}$ signal at Pumacocha and that $\delta^{18}O_{cal}$ variability is attributable to changes in the isotopic composition of precipitation.

SASM Variability and $\delta^{18}O_{precip}$. The principal control on $\delta^{18}O_{precip}$ over tropical South America is Raleigh-type fractionation during rainout (7). This is reflected by observations that show $\delta^{18}O_{precip}$ is more negative during the austral summer wet season, despite warmer temperatures, and more positive during the dry austral winter, when temperatures are generally cooler (12). There is, however, a slight offset of about 1–2 mo between the most intense precipitation and the most depleted $\delta^{18}O_{precip}$ at Pumacocha. Similar observations have been made in the Andes of Bolivia and attributed to rainout processes upstream over regions with slightly different precipitation seasonality (13). Hence $\delta^{18}O_{precip}$ is not simply a measure of precipitation amount at the site, but rather of the intensity of monsoon-related convective activity along the trajectory of an air mass (12–14). Year-to-year $\delta^{18}O_{precip}$ variability documented by observations, proxy data, and stable isotope-enabled global climate models show that $\delta^{18}O_{precip}$ is lower during intense monsoon seasons and vice versa (7). This isotopic response to monsoon variability is preserved and enhanced along an air mass trajectory, even if the precipitation signal at the site where stable isotopes are measured is not exactly the same as over the core region of convective activity, in this case the Amazon Basin (7). Hence the isotopic monsoon signal tends to be much more spatially coherent than monsoon precipitation, which is more strongly affected by microclimatic effects (14). This "isotopic memory" of an air mass and its influence on downstream $\delta^{18}O$ records like the one from Pumacocha means that local $\delta^{18}O_{precip}$ records reflect large-scale changes in the intensity of the SASM (7). We therefore interpret $\delta^{18}O_{cal}$ from Pumacocha as a proxy for the intensity of monsoon precipitation upstream.

Modern interannual variations in SASM intensity are caused by a number of factors. Pacific SST anomalies associated with El Niño–Southern Oscillation (ENSO) play a primary role in modulating SASM variability through changes in the Hadley and Walker circulation over tropical South America and the Pacific (15, 16). Changes in tropical Atlantic SSTs have also been linked to interannual variations in SASM activity and drought conditions over the Amazon Basin (15, 17). Soil moisture provides an important land surface feedback that has been shown to affect SASM precipitation patterns (18). All these factors lead to distinct variations in SASM activity, only loosely coupled to ITCZ variations over the tropical oceans on interannual time scales. Over the tropical Andes, summer precipitation is predominantly modulated by eastern equatorial Pacific SST (15). Cooling in the eastern equatorial Pacific (e.g., La Niña events) typically leads to reduced meridional baroclinicity and anomalous upper-level easterly flow over the Andes, which enhances near-surface moisture influx from the Amazon Basin, and vice versa. Therefore, although the SASM moisture supply lies almost exclusively in the tropical Atlantic, perturbations in atmospheric circulation caused by SST anomalies in the tropical Pacific play an important role mediating the intensity of the SASM in general and over the tropical Andes in particular (15).

SASM variability is less well understood on decadal and longer time scales because limited instrumental data in the tropics complicates investigations of long-term trends. Nonetheless, observa-

Fig. 4. (A) The Pumacocha $\delta^{18}O_{cal}$ record of SASM intensity. In B and C, the Pumacocha data are shown with a gray line for comparison with (B) $\delta^{18}O_{cal}$ from Cascayunga Cave, Peru, a record of lowland precipitation (22) and (C) $\delta^{18}O_{ice}$ from Quelccaya, Peru (23) smoothed with a 5-point moving average.

GEOLOGY

tions show that Atlantic SST variations play a significant role modulating SASM variability on multidecadal time scales (19). Paleoclimate studies similarly suggest that the tropical Atlantic may have been an important factor driving tropical South American rainfall variability on longer time scales and during past periods with different climatic boundary conditions (20, 21).

SASM Variability and Mean State Changes. Using the empirical relationships among Pumacocha $\delta^{18}O_{lw}$, $\delta^{18}O_{cal}$, and $\delta^{18}O_{precip}$, and the documented close relationship between SASM intensity and $\delta^{18}O_{precip}$ (7, 12), we interpret down-core variations in Pumacocha $\delta^{18}O_{cal}$ as representative of the intensity of the SASM. Accordingly, high $\delta^{18}O_{cal}$ is taken to reflect a less intense SASM, whereas lower $\delta^{18}O_{cal}$ represents a more intense SASM.

The Pumacocha $\delta^{18}O_{cal}$ record is characterized by considerable decadal-scale variability with three pronounced century-scale mean state changes during the MCA, LIA, and CWP, indicating major changes in the strength of the SASM (Fig. 4A). During the MCA, $\delta^{18}O_{cal}$ increased between A.D. 900 and 1100 with two distinct decadal-scale peaks from A.D. 935 to 950 and A.D. 1000 to 1040, indicating considerable reductions in SASM intensity. Medieval aridity was followed by a prolonged decrease in $\delta^{18}O_{cal}$ during the LIA starting as early as A.D. 1300, with minimum values between A.D. 1400 and 1820. This trend signifies the most dramatic increase in the strength of the SASM identified in the 2,300-year-long Pumacocha record. After A.D. 1820, $\delta^{18}O_{cal}$ generally increased to the present, especially after A.D. 1900. Between A.D. 1908 and 2007, $\delta^{18}O_{cal}$ increased from −15.0‰ to −12.9‰ at an average rate of 0.02‰ per year, which is the steepest and most rapid $\delta^{18}O_{cal}$ rise in the 2,300-year-long Pumacocha record. This increase reflects a long-term reduction in the intensity of the SASM that is similar in magnitude to the MCA aridity, but with a more abrupt onset.

Comparison with other highly resolved paleoclimate records from tropical South America shows that SASM mean state changes captured by the Pumacocha $\delta^{18}O_{cal}$ record were regional in scale with similar timing, direction, and magnitude. Specifically, the Pumacocha record tracks the 900-year-long Cascayunga Cave $\delta^{18}O_{cal}$ record (6.09 °S, 77.23 °W, 930 m asl), which is interpreted as a record of South American rainfall (Fig. 4B; ref. 22). The correspondence between these $\delta^{18}O$ records during their common period from A.D. 1050 to 2006 is notable because Cascayunga Cave is 3,400 m lower than Pumacocha and over 600 km to the north. Interestingly, the timing of mean state changes in the two records is nearly identical, although both the degree and magnitude of $\delta^{18}O$ variability are more pronounced in the Pumacocha record. Their similarities, however, support our contention that the Pumacocha record reflects regional scale precipitation variability and provides supporting evidence that strengthening of the SASM during the LIA was not strictly an Andean response.

The Pumacocha $\delta^{18}O_{cal}$ record also shares many features with the annually resolved Quelccaya Ice Cap $\delta^{18}O$ ($\delta^{18}O_{ice}$) record, which is approximately 500 km southwest of Pumacocha (13.93 °S, 70.83 °W; 5670 m asl; Fig. 4C; ref. 23). The timing and direction of mean state changes in these records are similar during the LIA and CWP, although the Quelccaya ice core shows greater variability and slightly later minimum $\delta^{18}O_{ice}$ values during the LIA. The MCA is less pronounced in the Quelccaya $\delta^{18}O_{ice}$ record than in the Pumacocha $\delta^{18}O_{cal}$ record, although $\delta^{18}O_{ice}$ increased between A.D. 980 and 1100 with two peaks centered on A.D. 990 and 1080. It is not clear why the MCA is less evident at Quelccaya because, although considerably lower resolution (100 years per sample), tropical Andean ice cores from Nevado Huascaran (24) and Sajama (25) have broadly elevated $\delta^{18}O_{ice}$ from A.D. 900 to 1300 and A.D. 900 to 1500, respectively. Notably, the Quelccaya $\delta^{18}O_{ice}$ record has historically been interpreted as a paleo-temperature record, although a number of authors have noted that precipitation amount likely plays a major

role driving $\delta^{18}O_{ice}$ variability (e.g., ref. 26). Because the Pumacocha and Cascayunga Cave records reflect SASM precipitation variations, their similarities with Quelccaya are consistent with the notion that Rayleigh distillation during rainout in the SASM region strongly influences isotopic records of tropical precipitation.

The close agreement in the timing, direction, and magnitude of mean state changes in $\delta^{18}O$ during the MCA, LIA, and CWP from lake sediment, speleothem, and ice core records supports the idea that a common large-scale mechanism influenced $\delta^{18}O$ reaching these central Andean sites spanning 11° latitude and 4,740 m of elevation. Based on the work presented here, the most likely cause of these documented shifts in $\delta^{18}O_{precip}$ is a change in SASM intensity as all three sites receive the majority of their annual precipitation during the monsoon season.

We compared the Pumacocha $\delta^{18}O_{cal}$ record to volcanic and solar radiative forcing (Fig. 5; e.g., 27, 28), reconstructed NH temperatures (29), variations in the latitude of the ITCZ (30, 31), and North Atlantic SST's (32, 33) to help identify the relevant factors that contributed to decadal variability and mean state changes in the SASM during the MCA, LIA, and CWP (Fig. 5). North Atlantic SST's are represented by the Mann et al. (32) reconstruction of SST from 60 °N to the equator and 75.5° to 7.5 °W and referred to generally as the North Atlantic. These variables were selected because numerous lines of evidence suggest that ocean–atmosphere processes, which are important drivers of modern SASM variability, contributed to past SASM changes

Fig. 5. (A) Reconstructed radiative forcing (blue) for the last 1,000 years from ref. 27 and residual ^{14}C for the last 2,300 years ($\Delta^{14}C$; a proxy for solar variability; red; ref. 28), (B) reconstructed Northern Hemisphere temperatures (29), (C) % Ti from the Cariaco Basin, Venezuela (30), interpreted as a proxy for the location of the ITCZ, and (D) reconstructed SST anomalies in the North Atlantic (32). The superimposed gray line in each of the graphs shows the Pumacocha $\delta^{18}O_{cal}$ record for comparison.

(e.g., ref. 34). Volcanic and solar forcing are included because changes in radiative forcing from these sources have been identified as leading influences on NH temperature variability during the MCA and LIA (27, 35), which model simulations suggest impact the tropical ocean–atmosphere systems, particularly in the North Atlantic (34, 36).

Immediately apparent from these comparisons is a remarkable correspondence between the Pumacocha $\delta^{18}O_{cal}$ record of SASM rainfall and reconstructed NH temperatures during the last 2,000 years (Fig. 5B). This relationship is particularly evident during the MCA, LIA, and CWP mean state changes. For example, the two greatest reductions in SASM intensity in the Pumacocha $\delta^{18}O_{cal}$ record were coincident with NH temperature maxima during the MCA and CWP. Conversely, the SASM was stronger than at any other point in the last 2,300 years when NH temperatures were at a 2,000-year low during the LIA. A cooling of the Northern Hemisphere leads to a southward displacement of the ITCZ, as documented in modeling and paleoclimate studies because of adjustments in the Hadley circulation balancing the need for enhanced northward heat transport (29, 30, 33). Although the Atlantic ITCZ serves as the main moisture conduit for SASM precipitation over the continent (37), the SASM and the marine ITCZ are separate systems, only loosely connected on interannual time scales (38). The remarkable similarities between the Pumacocha $\delta^{18}O_{cal}$ record and the reconstructions of both tropical SST's and the latitude of the ITCZ (29), however, suggest that the coupled tropical ocean–atmosphere system plays an important role in modulating SASM rainfall on decadal and longer time scales. This relationship is particularly apparent during the MCA, LIA, and CWP.

Weakening of the SASM observed in the Pumacocha $\delta^{18}O_{cal}$ record during the MCA is contemporaneous with generally elevated radiative forcing and warm NH temperatures (Fig. 5 A and B; ref. 29). At the same time, SST reconstructions from the North Atlantic show warmer, although variable, conditions (32, 33), whereas those from the equatorial Pacific indicate La Niña-like cooling (32). Although there is some debate regarding the tropical Pacific's response to radiative forcing, the available data support the occurrence of prolonged La Niña-like conditions during the MCA. Warm North Atlantic and cool eastern equatorial Pacific SSTs, as suggested by the proxy data, would shift the latitude of the ITCZ northward over both ocean basins (39, 40). In line with this model, elevated titanium concentrations (% Ti) in marine sediments from the Cariaco Basin off the coast of Venezuela occurred when North Atlantic SSTs peaked during the MCA, suggesting that the Atlantic branch of the ITCZ was persistently northward when the North Atlantic was warm (Fig. 5; ref. 30). Consistent with an intensification of the SASM when the ITCZ is shifted southward, the Pumacocha record shows that the SASM was considerably reduced during the MCA when peak % Ti in the Cariaco Basin record indicates that the ITCZ was persistently northward. The similarities between these records suggests that the northward shift in the ITCZ in response to tropical North Atlantic warming and eastern equatorial Pacific cooling during the MCA contributed to a reduction in the intensity of the SASM.

During the LIA, the Pumacocha $\delta^{18}O_{cal}$ record shows a strengthening of the SASM from A.D. 1400 to 1820 that was stronger than during any other period in the last 2,300 years. This strengthening occurred at the same time that diminished solar irradiance and elevated volcanism acted in concert to reduce radiative forcing and cool the NH (29, 35). Also during this interval, SST reconstructions show that the North Atlantic cooled (31) while the equatorial Pacific exhibited El Niño-like conditions (32). Proxy records of ITCZ variability from lakes in the western Pacific (31) and the Cariaco Basin (30) in the Atlantic indicate that the ITCZ was displaced considerably southward over both basins during the LIA (Fig. 5C). In the Atlantic, the southerly

ITCZ displacement is consistent with climate model simulations that show that NH cooling during the LIA would lower North Atlantic SSTs and strengthen the northern branch of Hadley Cell circulation, shifting the Atlantic ITCZ southward (34). The southerly position of the ITCZ over the Pacific and Atlantic during the LIA is coincident with the prolonged maximum in SASM rainfall documented by the Pumacocha record. This suggests that NH cooling and adjustments in the position of the ITCZ were more important in determining the mean state of the SASM during the LIA than enhanced El Niño-like conditions in the Pacific, which on interannual time scales tend to reduce rainfall over much of the SASM domain.

Increasing $\delta^{18}O_{cal}$ in the Pumacocha record after A.D. 1820 indicates a long-term weakening of the SASM, particularly after A.D. 1900. This reduction in SASM rainfall follows increases in radiative forcing (27), instrumental and reconstructed NH temperatures (29), and SSTs in the central equatorial Pacific and North Atlantic (32). These conditions are similar to those associated with weakening of the SASM during the MCA with the exception of apparent El Niño-like warming in the equatorial Pacific (32). The relationship between the Pumacocha record and reconstructed North Atlantic SSTs, evident even in the modern record, suggests that the weakened mean state of the SASM since the end of the LIA may be related to a northward shift in the Atlantic ITCZ in response to North Atlantic and NH warming.

Summary and Conclusions

The sedimentary $\delta^{18}O_{cal}$ record from Laguna Pumacocha provides an annually resolved view of variations in the isotopic composition of precipitation over tropical South America during the last 2,300 years. Changes in $\delta^{18}O_{precip}$ inferred from $\delta^{18}O_{cal}$ are attributed to variability in the intensity of SASM rainfall and show that the SASM experienced considerable variability at decadal scales with three pronounced century-scale mean state changes during the late Holocene: (i) a prolonged period of marked aridity during the MCA (A.D. 900–1100), (ii) a pronounced wet period during the LIA (A.D. 1400–1820), and (iii) an abrupt return to more arid conditions since A.D. 1900, a period characterized by the most significant and persistent positive $\delta^{18}O_{cal}$ trend in the entire 2,300-year record. The timing and direction of the mean state changes identified in the Pumacocha $\delta^{18}O_{cal}$ record are consistent with regional records from the Quelccaya Ice Cap and Cascayunga Cave, indicating that the Pumacocha record reflects large-scale trends in SASM rainfall, although the magnitude of variability within the lake sediment, ice, and speleothem records is quite different. Additionally, the similarities between these records supports recent work showing that rainfall variability is a major influence on isotopic records of tropical precipitation.

On decadal to century time scales, the Pumacocha $\delta^{18}O_{cal}$ record tracks reconstructed NH temperatures, north Atlantic SSTs, and latitudinal variability in the ITCZ. This suggests that SASM intensity is sensitive, in part, to latitudinal changes in the ITCZ on multidecadal time scales, likely mediated by NH surface temperatures and tropical SSTs. This idea is consistent with paleoclimate studies that document a relationship between North Atlantic SST and Andean effective moisture on millennial time scales (3, 4) and modern studies suggesting a tropical Atlantic influence on SASM variability. Despite our improved understanding of SASM rainfall variability during the MCA, LIA, and CWP, climate modeling studies and additional paleoclimate records of ocean and atmospheric conditions are needed to better define the relationships between SASM rainfall and ocean–atmosphere variability during the late Holocene. The results presented here, however, suggest that continued warming in the NH and North Atlantic might contribute to further weakening of the SASM. This is consistent with the sharp, persistent drop in SASM rainfall indicated by the Pumacocha $\delta^{18}O_{cal}$ record since A.D. 1900 and a long-term

GEOLOGY

decrease in mean rainfall over the Amazon Basin during the instrumental period from A.D. 1975 to 2003 (41). Given the anticipated loss of many tropical Andean glaciers within the next 50 years (42), sustained reductions in SASM rainfall could negatively impact the availability of water resources in the Andes and along the arid Pacific coast.

Materials and Methods

The Pumacocha data are archived at the National Oceanic and Atmospheric Administration Paleoclimatology World Data Center: ftp://ftp.ncdc.noaa.gov/pub/data/paleo/paleolimnology/southamerica/peru/pumacocha2011.txt.

Sediment Core Recovery. Sediment cores were retrieved from Pumacocha using a piston corer in 23.5-m water depth in June 2005 and August 2006. The composite 579.0-cm Holocene-length sediment record is comprised of successive overlapping 1-m-long drives. A network of freeze cores collected from the lake between 2006 and 2008 captured the undisturbed sediment–water interface (Table S5).

Age Control. Samples for ^{210}Pb, ^{226}Ra, and ^{137}Cs were measured at approximately 1 cm intervals between 0.0 and 30.0 cm from freeze core D-08 by direct gamma counting using an EG & G Ortec GWL high purity germanium well detector (Fig. S4 and Table S2). Eighteen radiocarbon (^{14}C) ages were determined by AMS on selected charcoal fragments (Table S1). The varve chronology is based on couplet counts from high-resolution digital images of freeze core B-08 and piston core C-06 to a depth of 103.5 cm. Four counts were performed on each core to ensure data quality and to derive an estimate of cumulative age error (1%).

Carbonate Sampling and Measurement. The uppermost 210 laminations were individually sampled from freeze cores B-08, B-07, and D-07 for carbonate isotope analysis. Piston cores C-06 and A-05 were sampled at 1-mm intervals. Samples were measured at the University of Arizona and the University of Pittsburgh. Results were calibrated to the standards NBS-19 and NBS-18 and are reported in conventional delta notation as the per mil (‰) deviation from Vienna Pee Dee Belemnite (VPDB) with 1σ precisions of ±0.1‰ for $\delta^{18}O_{cal}$ and $\delta^{13}C$. Replicate sample measurements yielded an internal sample reproducibility of ±0.02‰ for $\delta^{18}O_{cal}$ and ±0.03‰ for $\delta^{13}C_{cal}$.

1. Zhang P, et al. (2008) A test of climate, sun and culture relationships from an 1810-year Chinese cave record. *Science* 322:940–942.
2. Shanahan TM, et al. (2009) Atlantic forcing of persistent drought in West Africa. *Science* 324:377–380.
3. Abbott MB, Seltzer GO, Kelts KR, Southon J (1997) Holocene paleohydrology of the Tropical Andes from lake records. *Quat Res* 47:70–80.
4. Baker PA, et al. (2001) Tropical climate changes at millennial and orbital timescales on the Bolivian Altiplano. *Nature* 409:698–701.
5. Bowen GJ, Revenaugh J (2003) Interpolating the isotopic composition of modern meteoric precipitation. *Water Resour Res* 39:1299–1312.
6. Bowen GJ (2009) The online isotopes in precipitation calculator, version 2.2., http://www.waterisotopes.org.
7. Vuille M, Werner M (2005) Stable isotopes in precipitation recording South American summer monsoon and ENSO variability: Observations and model results. *Clim Dyn* 25:401–413.
8. Rozanski K, Araguás-Araguás L, Gonfiantini R (1992) Relation between long-term trends of oxygen-18 isotope composition of precipitation and climate. *Science* 258:981–985.
9. Kim S-T, O'Neil JR (1997) Equilibrium and nonequilibrium oxygen isotope effects in synthetic carbonates. *Geochim Cosmochim Acta* 61:3461–3475.
10. Rabatel A, Francou B, Jomelli V, Naveau P, Grancher D (2008) A chronology of the Little Ice Age in the tropical Andes of Bolivia (16 °S) and its implications for climate reconstruction. *Quat Res* 70:198–212.
11. von Gunten L, Grosjean M, Rein B, Urrutia R, Appleby P (2009) A quantitative high-resolution summer temperature reconstruction based on sedimentary pigments from Laguna Aculeo, central Chile, back to AD 850. *The Holocene* 19:873–881.
12. Vuille M, Bradley RS, Werner M, Healy R, Keimig F (2003) Modeling δ^{18}O in precipitation over the tropical Americas: 1. Interannual variability and climatic controls. *J Geophys Res* 108(D6):4174, 10.1029/2001JD002038.
13. Vimeux F, Gallaire R, Bony S, Hoffmann G, Chiang JCH (2005) What are the climate controls on dD in precipitation in the Zongo Valley (Bolivia)? Implications for the Illimani ice core interpretation. *Earth Planet Sci Lett* 240:205–220.
14. Schmidt G, LeGrande A, Hoffmann G (2007) Water isotope expressions of intrinsic and forced variability in a coupled ocean-atmosphere model. *J Geophys Res* 112:D10103.
15. Garreaud R, Vuille M, Compagnucci R, Marengo J (2009) Present-day South American climate. *Palaeogeogr Palaeoclimatol Palaeoecol* 281:180–195.
16. Marengo J, et al. (2008) The drought of Amazonia in 2005. *J Clim* 21:495–516.
17. Cox P, et al. (2008) Increasing risk of Amazonian drought due to decreasing aerosol pollution. *Nature* 453:212–215.
18. Collini E, Berbery E, Barros V, Pyle M (2008) How does soil moisture influence the early stages of the South American monsoon? *J Clim* 21:195–213.
19. Chiessi C, Mulitza S, Paetzold J, Wefer G, Marengo J (2009) Possible impact of the Atlantic Multidecadal Ocillation on the South American summer monsoon. *Geophys Res Lett* L21707.
20. Baker PA, Fritz SC, Garland J, Ekdahl E (2005) Holocene hydrologic variation at Lake Titicaca, Bolivia/Peru, and its relationship to North Atlantic climate variation. *J Quat Sci* 20:655–662.
21. Baker PA, et al. (2001) The history of South American tropical precipitation for the past 25,000 years. *Science* 291:640–643.
22. Reuter J, et al. (2009) A new perspective on the hydroclimate variability in northern South America during the Little Ice Age. *Geophys Res Lett* 36:L21706.
23. Thompson LG, Thompson EM, Dansgaard W, Groots PM (1986) The Little Ice Age as recorded in the stratigraphy of the tropical Quelccaya Ice Cap. *Science* 234:361–364.
24. Thompson LG, et al. (1995) Late Glacial Stage and Holocene Tropical Ice core records from Huascaran, Peru. *Science* 269:46–50.
25. Thompson LG, et al. (1998) A 25,000-year tropical climate history from Bolivian ice cores. *Science* 282:1858–1864.
26. Hastenrath S, Polzin D, Francou B (2004) Circulation variability reflected in ice core and lake records of the southern tropical Andes. *Clim Change* 64:361–375.
27. Crowley TJ (2000) Causes of climate change over the past 1000 years. *Science* 289:270–277.
28. Bard E, Raisbeck G, Yiou F, Jouzel J (2000) Solar irradiance during the last 1200 years based on cosmogenic nuclides. *Tellus B Chem Phys Meteorol* 52:985–992.
29. Moberg A, Sonechkin DM, Holmgren K, Datsenko NM, Karlen W (2005) Highly variable Northern Hemisphere temperatures reconstructed from low- and high-resolution proxy data. *Nature* 433:613–617.
30. Haug GH, Hughen K, Sigman DM, Peterson LC, Rohl U (2001) Southward migration of the intertropical convergence zone through the Holocene. *Science* 293:1304–1308.
31. Sachs JP, et al. (2009) Southward movement of the Pacific intertropical convergence zone AD 1400–1850. *Nat Geosci* 2:519–525.
32. Mann ME, et al. (2009) Global signatures and dynamical origins of the Little Ice Age and Medieval Climate Anomaly. *Science* 326:1256–1260.
33. Keigwin LD (1996) The Little Ice Age and Medieval warm period in the Sargasso Sea. *Science* 274:1504–1508.
34. Broccoli AJ, Dahl KA, Stouffer RJ (2006) Response of the ITCZ to Northern Hemisphere cooling. *Geophys Res Lett* 33:L01702.
35. Jones PD, Mann ME (2004) Climate over past millennia. *Rev Geophys* 42:RG2002, 10.1029/2003RG000143.
36. Mann M, Cane M, Zebiak S, Clement A (2005) Volcanic and solar forcing of the tropical Pacific over the past 1000 years. *J Clim* 18:447–456.
37. Marengo J, et al. (2010) Recent developments on the South American monsoon system. *Int J Climatol*, 10.1002/joc.2254.
38. Garcia S, Kayano M (2010) Some evidence on the relationship between the South American monsoon and the Atlantic ITCZ. *Theor Appl Climatol* 99:29–38.
39. Enfield DB, Mayer DA (1997) Tropical Atlantic sea surface temperature variability and its relation to El Niño-Southern Oscillation. *J Geophys Res* 102:929–945.
40. Takahashi K, Battisti DS (2007) Processes controlling the mean tropical Pacific precipitation pattern. Part 1: The Andes and eastern Pacific ITCZ. *J Clim* 20:3434–3451.
41. Villar JCE, et al. (2008) Spatio-temporal rainfall variability in the Amazon Basin countries (Brazil, Peru, Bolivia, Colombia, and Ecuador). *Int J Climatol* 29:1574–1594.
42. Vuille M, et al. (2008) Climate change and tropical Andean glaciers: Past, present, and future. *Earth Sci Rev* 89:79–96.